Boron removal and reinsertion studies in ^{10}B-^{11}B exchanged HAMS-1B (H-[B]-ZSM-5) borosilicate molecular sieves

Andrea Hough[1a,c], Alexander F. Routh[1a, c], Stuart M. Clarke[1b,c]

Paul V. Wiper[2], Luís Mafra[2], Jeffrey Amelse[2]

[1a] Departments of Chemical Engineering and Biotechnology, [1b] Chemistry, and [1c] The BP Institute. Cambridge University, Cambridge, U.K.
[2] Department of Chemistry, CICECO, University of Aveiro, 3810-193 Aveiro, Portugal
[3] BP Amoco Chemical Company 150 W. Warrenville Road, Naperville, IL 60563 USA

Abstract

Boron removal from and reinsertion into the framework of a HAMS-1B (H-[B]-ZSM-5) borosilicate molecular sieve was studied by a combination of wet chemistry and ^{11}B solid-state NMR (SSNMR) spectroscopy. Uncalcined HAMS-1B shows only tetrahedral boron. However, three boron species are observed in the NMR spectra of as-prepared and then calcined HAMS-1B-3: tetrahedral framework boron ($^{[4]}B_{fr}$), trigonal framework boron ($^{[3]}B_{fr}$), and non-framework trigonal boron ($^{[3]}B_{NF}$). A picture has emerged as to the origins of these three species. Trigonal boron species are formed via hydrolysis by reaction with the water formed from water release and water formed by oxidation and removal of the template during calcination. $^{[3]}B_{NF}$ is confirmed to be due to free boric acid formed by complete removal of boron from the framework. The trigonal boron species are readily removed from the framework by slurrying in water or mild acid solutions. Tetrahedral boron remains at a concentration about equal to that in the calcined sieve, indicating that it is more difficult to remove. The extent of boron removal and reinsertion is pH dependent. Boron is removed to a greater extent at low pH and can be reinserted when pH is increased. Boron reinsertion into the framework is proven by ^{11}B SSNMR of a series of ^{10}B-^{11}B exchanged borosilicate zeolites. Surprisingly, when boron is reinserted it enters as tetrahedral boron, not trigonal boron, thus reversing the partial hydrolysis and removal during calcination.

1. Introduction

Borosilicate zeolites are an interesting class of molecular sieves due to their inherent sensitivity towards hydration/dehydration treatment. It is well established that boron undergoes a geometry transformation from tetrahedral to trigonal upon dehydration, reported by Koller [4], Fild [5,6], S.-J. Hwang, et al. [7]. The resulting transformation renders the sieve as a weak Brønsted acid catalyst.

In a recent work, Wiper *et al.* studied the Brønsted/Lewis acid properties of a

dehydrated HAMS-1B borosilicate molecular sieve by multinuclear Solid State Nuclear Magnetic Resonance Spectroscopy (SSNMR) [2]. They found that the material exhibits weak Brønsted acidity and strong Lewis acidity. These findings are consistent with the model for boron hydrolysis and removal from the framework proposed by de Ruiter *et al.* [3]. For the sake of clarity, this model is repeated here in Scheme 1.

Scheme 1.

In the present contribution, as well as in other reports [2,4-7], the ^{11}B MAS NMR spectrum of calcined HAMS-1B (or H-[B]-ZSM-5) samples may present multiple boron species depending on level of hydration/dehydration. These species are designated here as: tetrahedral framework boron ($^{[4]}B_{fr}$), trigonal framework boron ($^{[3]}B_{fr}$), and non-framework trigonal boron ($^{[3]}B_{NF}$). The tetrahedral framework boron ($^{[4]}B_{fr}$) species is associated with a bridging hydroxyl (Si-OH-B) Brønsted acid site, similar to the Si-OH-Al acid site in the aluminosilicate HZSM-5. In borosilicates, the bridge is easily broken by dehydration at elevated temperature. This explains why unsupported borosilicate molecular sieves have little intrinsic activity for many hydrocarbon conversion reactions requiring strong Brønsted acidity and high reaction temperatures.

The bridging hydroxyl is shown in the far upper left in Scheme 1. Successive dehydration leads to the various trigonal framework boron species, with final boron removal leading to free boric acid shown in the far lower right. Not all of the trigonal boron species can be distinguished by 1D Hahn echo boron NMR due to resonance overlapping [7]. Boron hydrolysis and removal leads to silanol groups with complete removal leading to silanol nests whose protons give rise to a resonance at 1.7 ppm in ^{1}H NMR spectra [2]. Rehydration (upper line in Scheme 1 moving to the left) leads to the mending of the "broken bridges", which leads to an enhancement of the ^{11}B NMR signal associated with $^{[4]}B_{fr}$ sites. Here water acts as a weak base. The enhancement of the $^{[4]}B_{fr}$ signal is even larger when a strong base, such as timethylphosphine oxide is adsorbed [2].

While unsupported HAMS-1B has little intrinsic activity, it becomes activated when supported on alumina, and alumina supported HAMS-1B borosilicate molecular sieve exhibits excellent activity and shape selectivity as a catalyst for EB conversion/xylene isomerization reactions of importance in the commercial production of para-xylene [8,9].

In recent years, Zones and co-workers have focused research on creating new, novel borosilicates zeolite topologies in addition to studying the post-modification of borosilicates to replace framework boron by framework aluminum or gallium [12-15]. For example, they found that boron in the framework of large pore molecular sieves can be replaced by aluminum by treating large pore borosilicate molecular sieves with aluminum nitrate solutions under reflux. However, they have concluded that this technique does not work for medium pore borosilicate molecular sieves (such as boron MEL), and speculate that hydrated Al^{+3} is too large to enter medium pores [14, 15].

Amelse and coworkers had previously concluded that aluminum does not enter the framework of HAMS-1B when it is activated by supporting on alumina from the absence of an band at 3610 cm^{-1} in the infrared spectra which has been associated with the bridging hydroxyl (Si-OH-Al) in ZSM-5 [16, 17]. This band is readily observed in ZSM-5 aluminosilicate molecular sieves and alumina supported ZSM-5 down to very low levels of framework aluminum. However, the band is not observed in alumina supported HAMS-1B catalysts having activity equal to or greater than ZSM-5 catalysts prepared from ZSM-5 having over 1 Al/ unit cell. The exact nature of the aluminum species that activates HAMS-1B when it is supported on alumina remains the subject of current research.

In this work, the complete removal of boron from and reinsertion into the framework of HAMS-1B is studied by a combination of wet chemistry and ^{11}B SSNMR spectroscopy. We find that boron in calcined HAMS-1B is readily removed by exposure to acidic aqueous solutions, and that it can be reinserted after removal by increasing the pH of the treating solution. The extent of boron removal is dependent on the pH of the treating solution, with more boron removed at lower pH. Trigonal framework boron, believed to be formed during sieve calcination, is most easily removed. Surprisingly, we find

that when boron is reinserted by increasing the pH, it reinserts as tetrahedral boron. Thus, boron removal and reinsertion provides a method for repairing partial boron removal or conversion to trigonal species during calcination. Proof of reinsertion is provided by a SSNMR study of ^{10}B – ^{11}B exchange experiments. Finally, we propose a model to explain the three boron species observed in calcined HAMS-1B.

2. Experimental Section

Synthesis of HAMS-1B

The AMS-1B borosilicate molecular sieve is disclosed in M. R. Klotz, U.S. Patent 4,269,813 (1981). AMS-1B has the MFI framework type designated by the Structure Commission of the International Zeolite Association [1]. ZSM-5 is the aluminosilicate analog of MFI sieves, and silicalite is the all silica analog. The hydrogen form of AMS-1B, designated as HAMS-1B can be formed directly after calcination without the need for exchange, from gels substantially free of alkali metals following the disclosure of M. S. Haddad in U.S. 5,053,211 (1991). HAMS-1B is often referred to in the literature as H-[B]-ZSM-5.

HAMS-1B Enrichment with ^{10}B and ^{11}B isotopes

HAMS-1B samples were prepared from boric acid having a natural abundance of ^{10}B and ^{11}B from boric acid obtained from Sigma-Aldrich. Natural abundance is 19.9 atom% ^{10}B and 80.1% ^{11}B. The sample with natural abundance is the same sample studied in our previous paper [2]. Sigma-Aldrich also supplied boric acid enriched in ^{10}B and ^{11}B (greater than 99 atom % isotopic purity). However, due to limited current stock of ^{11}B boric acid at the time, some additional material was ordered from American Elements, Los Angeles, CA (www.americanelements.com).

Boron incorporation leads to a shrinkage of the MFI unit cell, and framework boron content can be determined by XRD following the method outlined by Meyers, et al. [10]. XRD indicated that all samples of HAMS-1B studied here were essentially 100% crystalline. The sample prepared from natural abundance boron boric acid had a B/uc (uc=unit cell) as measured by XRD of 5.0-5.4, based on several measurements. The aluminum content (present from the starting silica sol) was about 350 ppm. A framework boron content of 5.4 B per 96 T-atoms per unit cell corresponds to a Si/B ratio of 16.8. It is interesting to note that this approaches the minimum Si/Al ratio of 12.5 reported for HZSM-5. Thus, the MFI framework is able to support the incorporation of about as many boron atoms as aluminum atoms.

Total boron content for the ^{10}B and ^{11}B HAMS-1B samples were 1.24 and 1.22 wt% respectively, and framework boron content was determined to be 5.2 and 4.6 B/uc via XRD respectively.

SSNMR Measurements

^{11}B magic-angle spinning (MAS) nuclear magnetic resonance (NMR) spectra were acquired on a Bruker Avance III 400 wide bore spectrometer operating at a B_0 field of 9.4 T with ^{1}H, and ^{11}B Larmor frequencies of 400.1, and 104.3 respectively. A MAS rate of 15 kHz was used for all experiments. The samples were packed into a 4 mm outer diameter ZrO_2 rotor using a double resonance probe.

^{11}B MAS NMR spectra were recorded using a Hahn-echo with a 90^{o} and a 180^{o} soft pulses of 12 μs and 24 μs, respectively employing a rf field strength of 20.8 kHz and rotor-synchronised echo delays of 1 rotor period (66.6 μs). A Hahn-echo experiment was performed to remove the ^{11}B probe background signal, which is present in most of the commercial probe heads. The simulation of the NMR spectra was carried out using the program dmfit [11]. Errors associated to fittings are between 1-2 %. Chemical shifts are quoted in ppm using a secondary reference of 0.1 M aqueous solution of H_3BO_3 (19.6 ppm).

Wet Chemistry Procedures

The HAMS-1B sieves were slurried in aqueous solutions as follows.

Slurries of 1 wt% HAMS-1B in distilled water were prepared in polypropylene bottles. The solutions were agitated for one hour. pH was measured by via a pH meter. The pH of the slurries ranged from 3.5 to 4.5. The sieves were filtered using Millipore 0.1 μm Millex or Sterifil filters. The filtrates were confirmed to be free of sieve particles by dynamic light scattering. The sieves were dried at 80 °C for one hour. Sieves and/or filtrates were analyzed for boron by Inductively Coupled Plasma- Atomic Emission Spectra (ICP-AES) at the Department of Earth Sciences, University of Cambridge or at the BP Research Center in Naperville, IL.

3. Results and Discussion

3.1. Boron Removal and Reinsertion Followed By Wet Chemistry

Boron removal and reinsertion as a Function of pH was studied via the following experiments. Results are summarized in Figure 1.

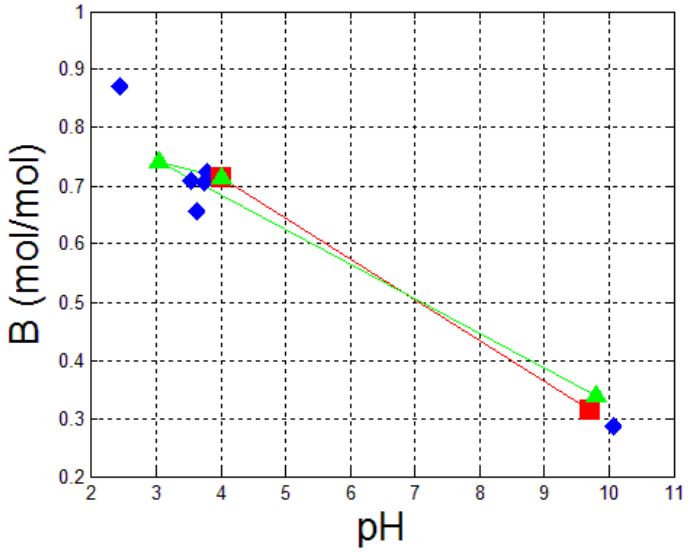

Figure 1. Boron in the filtrate relative to boron in the starting calcined HAMS-1B sieve.
Blue = Preparations (a): Dispersed in water, dilute acetic acid or dilute ammonium hydroxide.
Red = Preparations (b): Disperse in water then swung to high pH.
Green = Preparations (c): Dispersed in water, swing to low pH, then to high pH.

For clarity, these experiments are described in detail below, and shown pictorially in Figure 2.

Preparations (a): The blue diamonds in Figure 1 represent preparations (a) where HAMS-1B was dispersed in water, dilute acetic acid, and dilute ammonium hydroxide to achieve different final pH. For these preparations, the acidic, basic or neutral (water) solutions were prepared first, before adding the sieve. Roughly 70% of the total boron in the starting HAMS-1B enters the filtrate when dispersed as a 1 wt% sieve slurry in distilled water (pH near 3.5). When dispersed in dilute acetic acid to achieve a final pH near 2.3, more boron enters the filtrate (nearly 87%). When dispersed in dilute ammonium hydroxide to achieve a final slurry pH of about 10, only about 30% of the boron is found in the filtrate.

Preparations (b): The red squares and line represent preparations (b), where HAMS-1B was dispersed in distilled water before its pH is raised to 10. Consistent with prior preparation (a) experiments, exposure to water led to about 70% of the boron leaving the sieve and entering the liquid phase. When the pH is raised to 10, the filtrate is found to contain only about 30% of the boron from the starting sieve, about the same as dispersing in a basic solution of the same pH without first dispersing at low pH. This experiment indicates that boron removed at low pH was re-deposited on the solids when the pH was increased.

Preparations (c): The green triangles and line represent preparations (c), where HAMS-1B was first slurried in distilled water. pH was then lowered to 3 by adding dilute acetic acid, and finally raised to 10 by adding dilute ammonium hydroxide. Consistent with the prior experiments for preparations (a) and (b) , exposure to low pH led to a high fraction of the boron (about

74%) exiting the sieve into the liquid phase. When pH was increased to 10, once again, the filtrate contained only about 30% of the boron from the starting sieve, indicating that boron had re-deposited on the sieves.

The experiments in this section clearly indicate that boron removed at low pH is re-deposited at high pH, and the amount of boron removal into the filtrate is a function of final pH.

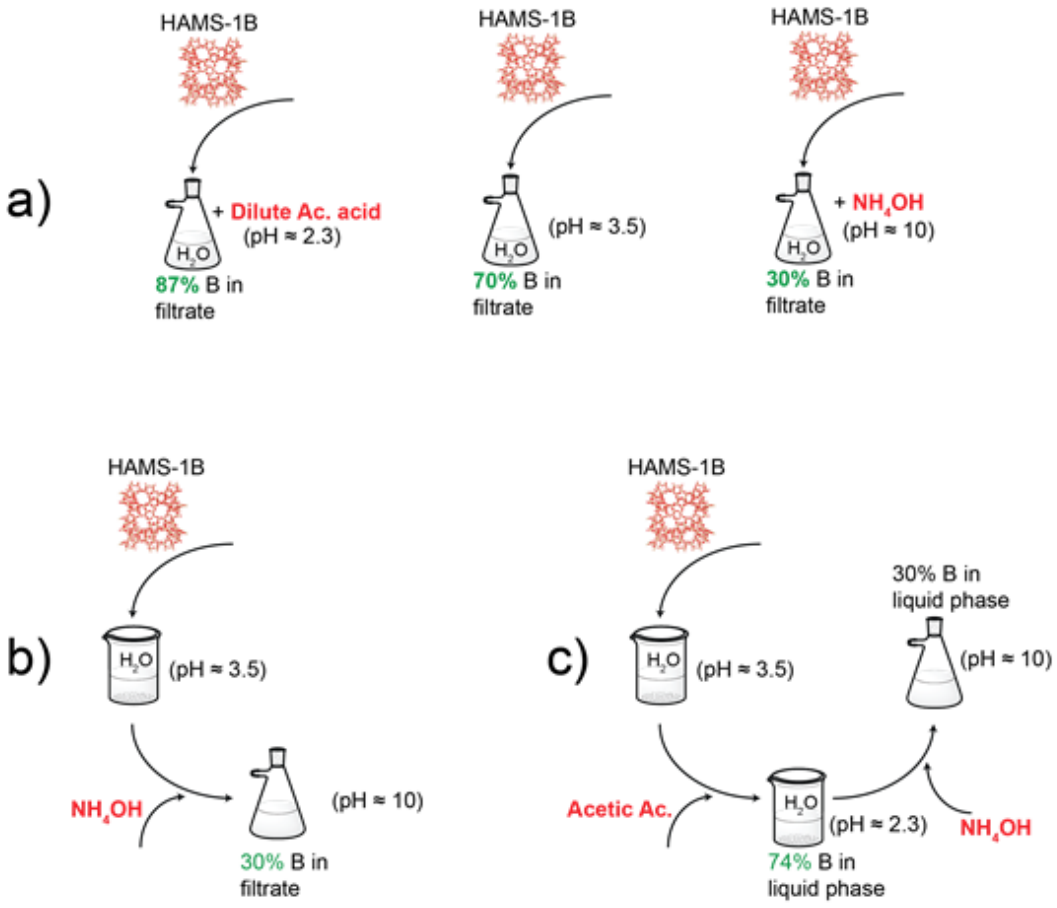

Figure 2. Schematic representation of the wet chemistry processes to investigate boron removal and reinsertion in HAMS-1B as a function of pH. Boron content and pH in filtrate of HAMS-1B dispersed in: **a)** water, dilute acetic acid and dilute ammonium hydroxide (from left to right); **b)** water then swung to high pH; **c)** water, swung to low pH, then to high pH.

Following Boron Removal and Re-Insertion by SSNMR of ^{10}B-^{11}B Exchanged Samples

In the previous section, it was shown that boron is removed at low pH, and is re-deposited on/in the sieve when pH is increased. However, *it does not prove that boron is re-inserted into the framework*. In this section, we prove the latter by studying ^{10}B-^{11}B exchange in HAMS-1B prepared from isotopically pure (>99 atom%) ^{10}B- and ^{11}B-boric acid. The entire process is

illustrated in Figure 3.

The boron natural abundance HAMS-1B (Sample 1), and HAMS-1B prepared from isotopically pure ^{10}B (Sample 2) and ^{11}B (Sample 3) boric acid were dispersed in distilled water to form a 1 wt% slurry of HAMS-1B. 150 g of each slurry was prepared. The sieves were filtered, dried for 1 hour at 80 ºC, and then analyzed for boron content by ICP. The water-treated and dried sieves from Samples 1, 2, and 3 are designated as Samples 4, 5, and 6 respectively (See Figure 3). Consistent with the results from Section 3.1, Samples 4, 5, and 6 were found to be deboronated (See ICP data in Table 1).

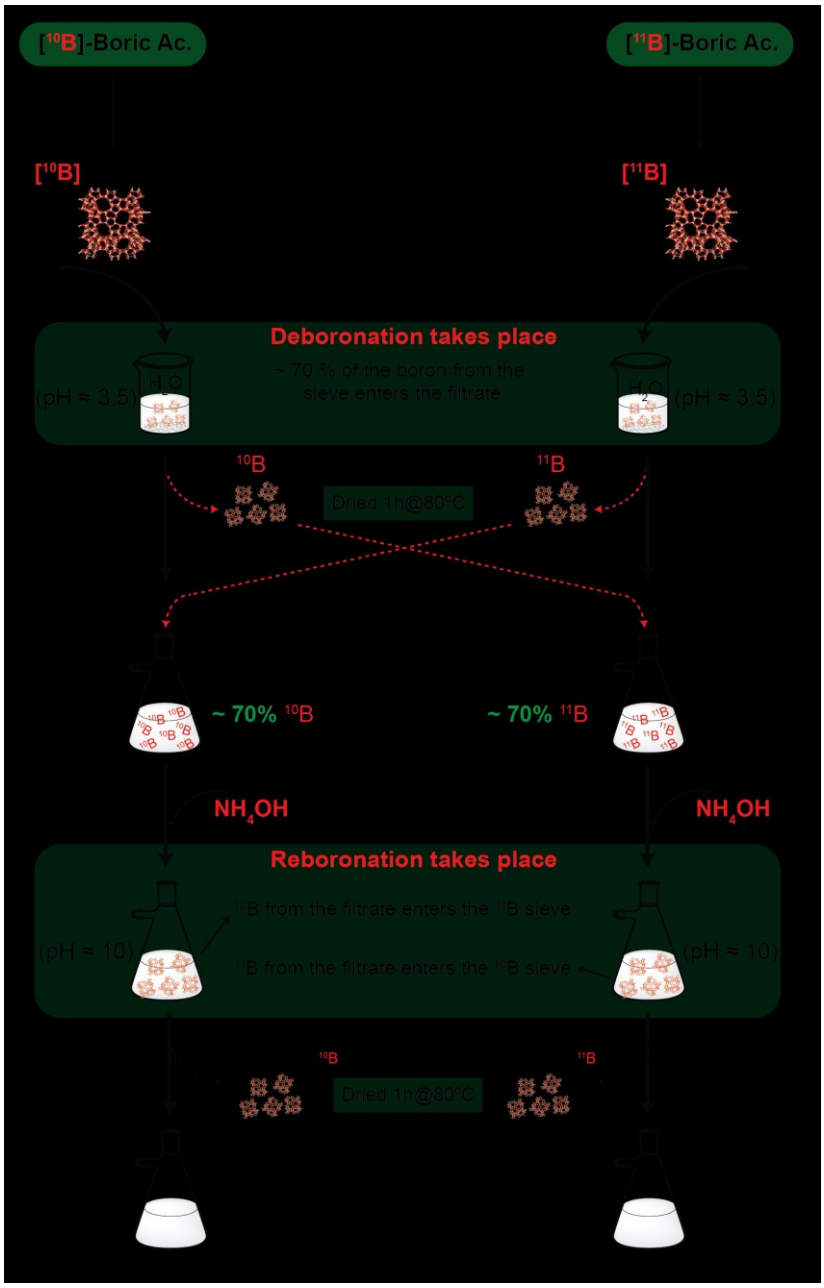

Figure 3. Schematic representation of the boron removal and re-insertion procedure of ^{10}B-^{11}B exchanged HAMS-1B samples 2 and 3 to generate the final treated HAMS-1B samples 7 and 8.

In parallel experiments, HAMS-1B prepared from isotopically pure ^{10}B (Sample 2) and ^{11}B (Sample 3) boric acid were dispersed in distilled water to form 150 g each of 1 wt% slurries of HAMS-1B, as previously described. The slurries were agitated for 1 hrand then filtered. The deboronated filtered solids were dried in air at 80 ºC for one hour. This time, the filtrates were retained. The dried sieves and filtrates were crossed, i.e., the deboronated sieve prepared from the ^{10}B sieve was exposed to the filtrate obtained by deboronation of the ^{11}B sieve, and vice versa. Re-deposition of boron was caused to take place by adding ammonium hydroxide to increase the pH to 10. Thus, ^{11}B from the filtrate was deposited on the ^{10}B deboronated sieve, and vice versa. The deboronated solids from the original ^{10}B enriched sieve onto which ^{11}B was deposited was labelled Sample 7, and the deboronated solids from the original ^{11}B enriched sieve onto which ^{10}B was deposited was labelled Sample 8. (See Figure 3).

To be precise, 0.8 g of the dried deboronated sieve (Sample 5) prepared from the ^{10}B-enriched starting sieve (Sample 2) was slurried in 79.2 g of the filtrate obtained by deboronating the ^{11}B-enriched starting sieve (Sample 3). pH was increased to 10 by adding 0.4 g ammonium hydroxide to deposit ^{11}B from the filtrate onto/into the ^{10}B deboronated sieve. The mixture was agitated for 30 min before the solids were filtered and dried at 80 ºC for one hour and designated as Sample 7

Similarly, the ^{11}B sieve that had been deboronated by slurrying in distilled water was filtered, dried (Sample 6), exposed to the filtrate from the slurry of the ^{10}B-enriched sieve in distilled water, and finally pH was increased to 10. After agitating for 30 minutes the solids were filtered, and dried at 80 ºC for one hour. These solids are designated as Sample 8 (See Figure 3).

Boron content of samples 1-8 were determined by ICP, with results presented in Table 1. Samples 1-3, 6, and 7 were analyzed by ^{11}B SSNMR. The ^{11}B Hahn-echo NMR spectrum of Sample 2 showed only a very minor blip when magnified 10 fold due to ^{11}B impurity in this sample prepared from ^{10}B boric acid. This proves that only the ^{10}B isotope is present within Sample 2 as the ^{10}B nucleus cannot be detected with the NMR probe tuned at the ^{11}B frequency as they (^{10}B and ^{11}B) resonate at very distinct Larmor frequencies.

The ^{11}B Hahn-echo MAS NMR spectra of Samples 3, 6, and 7are provided in Figure 4.

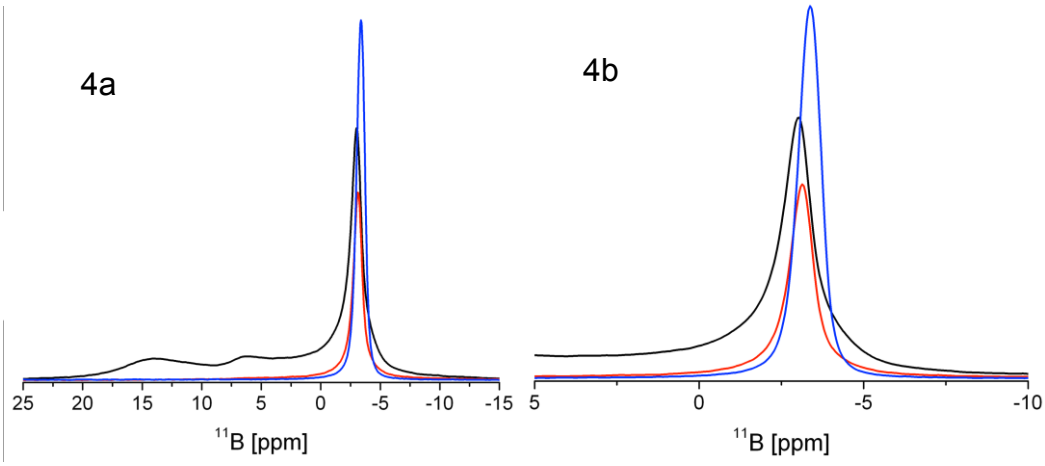

Figure 4. 4a: ^{11}B Hahn echo SS NMR spectra of from top to bottom (Sample 7, **Blue**); (Sample 3, **Black**), and (Sample 6, **Red**). 4b: Zoom of the tetrahedral near -2 ppm.

A deconvolution of boron species in the spectrum of the HAMS-1B prepared from ^{11}B boric acid, as synthesized and calcined (Sample 3), is provided in Figure 5.

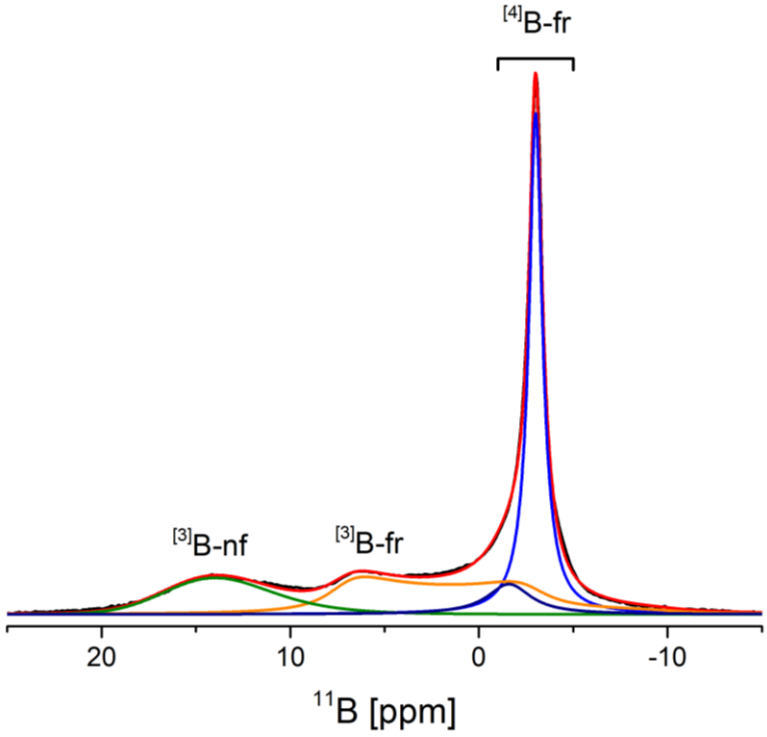

Figure 5. ^{11}B Hahn-echo MAS NMR spectra of hydrated Sample 3 and deconvolution of individual components and overall simulated fit (red line) are also shown based on the 2D ^{11}B 3QMAS experiment shown in Figure 6. The fitting models and parameters obtained from deconvolution of the spectrum are: Gaussian/Lorentzian δ_{iso} -3.0 and -1.6 ppm. Quadrupolar line shape: δ_{iso} 10 ppm, C_Q 2.3 MHz, η 0.2 and Czjzek line shape: δ_{iso} 16 ppm, δ_{iso} 5.2 ppm, C_Q 1.2 MHz.

Justification for using 4 species to fit the spectrum of Figure 5 comes from Figure 6, which shows 2D ^{11}B 3QMAS NMR spectra of “hydrated” (left) and

"dehydrated" (right) HAMS-1B. The spectrum in the anisotropic dimension (along the Y-axis) of hydrated Sample 1, plus the contours in the 2D plot show the presence of strong and weak tetrahedral peaks.

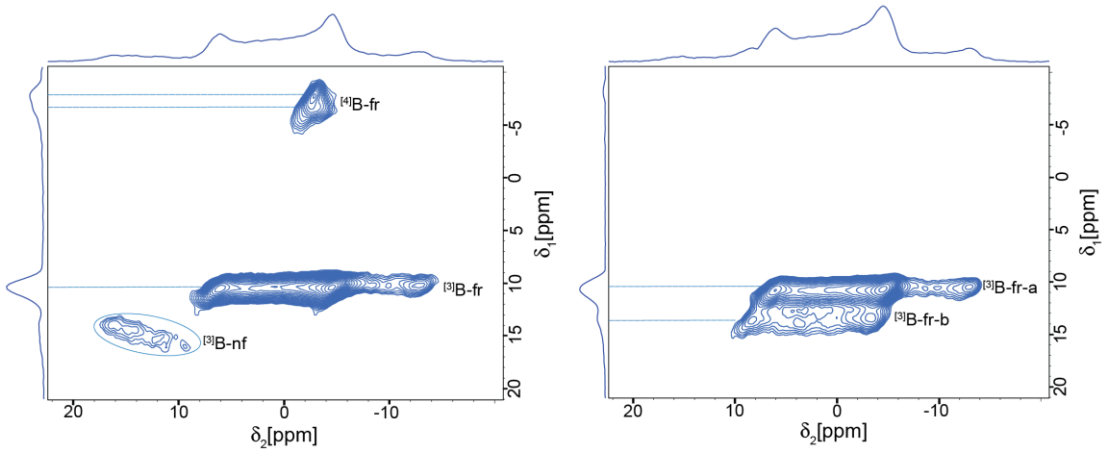

Figure 6. ^{11}B 3QMAS NMR spectra of "hydrated" (left) and "dehydrated" (right) HAMS-1B (Sample 1 in Table 1).

Table 1. ICP boron concentration and relative boron species concentrations as determined from deconvolution of the ^{11}B Hahn-echo MAS NMR spectra.

					NMR species fraction			
Sample no.	**ICP Boron Content wt%**	**Starting Sieve Description**	**Treatment**	**Relative $^{[4]}$B-fr peak intensity**	**$^{[4]}$B-fr**	**$^{[3]}$B-fr**	**$^{[3]}$B-nf**	**Total Framework Boron wt %**
1	1.03	Natural abundance HAMS-1B	As calcined after synthesis					
2	1.24	HAMS-1B from ^{10}B boric acid						
3	1.22	HAMS-1B from ^{11}B boric acid		100	47	36	17	1.01
4	0.37	Natural abundance HAMS-1B	Dispersed as 1wt% in water					
5	0.33	HAMS-1B from ^{10}B boric acid						
6	0.35	HAMS-1B from ^{11}B boric acid		75	100			0.43
7	0.76	HAMS-1B from ^{10}B boric acid	No.5 exposed to filtrate from No.6, then pH to 10	140				0.80
8	0.68	HAMS-1B from ^{11}B boric acid	No.6 exposed to filtrate from No.5, then pH to 10					

Thus, the experimental spectrum in Figure 5 was fitted using four components: two Gaussian components centered at -3.0 and -1.6 ppm assigned to $^{[4]}B_{fr}$ units; one 2nd order quadrupolar lineshape centered at ca. 3.0 ppm (isotropic chemical shift = δ_{iso} = *10 ppm*) assigned to $^{[3]}B_{fr}$ units and one simulated peak using the Czjzek model centered at *ca.* 14 ppm (δ_{iso} = *16 ppm*). The latter signal was fitted using this model because of site distribution along the quadrupolar induced shift (QIS) axis shown by the contour

lineshape indicated by the blue circle from the ^{11}B MQMAS NMR spectrum (Figure 6). The fact that the site at δ_{iso} = 16 ppm exhibits a lineshape extended along an axis (QIS) with negative slope suggests that the boron nucleus is in a disordered environment. We tentatively assign this site to $^{[3]}B_{NF}$ species of the type $B(OH)_3$, consistent with the assignment from Hwang *et al.*[7]. This assignment is based upon comparing the ^{11}B MQMAS NMR spectrum of hydrated and dehydrated HAMS-1B, shown in Figure 6. Upon dehydration, the $^{[4]}B_{fr}$ sites convert to $^{[3]}B_{fr}$, which we have previously assigned [2]. Notice how the lineshapes of the $^{[3]}B_{fr}$ sites lie flat along the F2 axis in both hydrated and dehydrated HAMS-1B. Therefore, if additional trigonal framework sites appear, they should have similar quadrupolar parameters and contour lineshapes. The fact that the site at 16 ppm, in the hydrated HAMS-1B sample, exhibits a lineshape extended along an axis (QIS) with negative slope suggests that this boron site is disordered. The quadrupolar parameters obtained from simulation for boron sites within hydrated and dehydrated HAMS-1B are given within the figure caption. Note that in 2D spectrum of the dehydrated sample (Right side of Figure 6) two of three possible trigonal boron species (on the right side of lines 1-3 of Scheme 1) are observed. It is possible that the parameters for the species on the right side of lines 2 and 3 overlap. Note also that only one of these species is observed in the hydrated specimen (Left side of Figure 6).

The relative boron species concentrations as estimated from deconvolution of the^{11}B Hahn-echo MAS NMR spectra are provided in Table 1. The HAMS-1B prepared from the ^{11}B boric acid (Sample 3) contains about 47% of $^{[4]}B_{fr}$, 36% of ($^{[3]}B_{fr}$), and 17% of $^{[3]}B_{NF}$. The total $^{[4]}B_{fr}$ and $^{[3]}B_{fr}$ boron content is about 1.01 wt% ((1-0.17)x1.22 wt%). This is about the same level as has been observed for many HAMS-1B samples that have been carefully prepared and carefully washed after recovering the as-synthesized solids from the BP laboratory.

Using Sample 3 as a reference, the framework boron content of the other samples can be estimated based on the relative NMR peak intensities. These values are provided in the far right hand column of Table 1. For example, the estimated framework boron content of Sample 6 is 1.22% total B for Sample 3 x 0.47 (percent of total NMR area of $^{[4]}B_{fr}$) x 75/100 = 0.43 wt%. The ICP total boron content for Sample is 0.35 wt%, a bit lower than that estimated from NMR, but probably within uncertainty.

Similarly the total framework boron content estimated by NMR for Sample 7 is 1.22 x 0.47 x 140/100 = 0.80 wt%. One might ask: What happened to the roughly 30% of the ^{10}B expected to remain in the sieve following initial slurrying in water? It is possible that some exchange of this ^{10}B in the framework took place when exposed to the ^{11}B containing filtrate.

No $^{[3]}B_{NF}$ site is observed in samples after slurrying in distilled water at 1 wt% solids. Thus, this treatment seems to be effective at removing such species.

In an attempt to prove that the $^{[3]}B_{NF}$ is boric acid, representing complete removal of this boron from the framework, the spectra of boric acid impregnated ZSM-5 was compared to HAMS-1B at two different magnetic

fields (400 and 800 MHz) as shown in Figure 7. A Zeolyst ZSM-5 obtained in the ammonium form (Zeolyst CBV 3024E, lot 2439-33, Vendor reported SAR = 32, ICP Al = 2.4 wt%) was first calcined to drive off ammonia, and was then impregnated to the point of incipient wetness to obtained a treated sieve containing about 0.35 wt% B by ICP.

The spectra (Figure 7) show that the boric acid impregnated ZSM-5 sample presents an intense ^{11}B resonance coincident with the $^{[3]}B$-nf in HAMS-1B. Thus, it does indeed appear that the $^{[3]}B$-nf in HAMS-1B is boric acid. Note that these spectra suggest that some boron can enter the framework of ZSM-5. It might appear that incorporation is significant from the spectrum at 400 MHz. However, this is due to the fact that the $^{[3]}B$-fr and $^{[4]}B$-fr are riding on top of the lines due to $^{[3]}B$-nf. At 800 MHz, the spectral contributions of these species are better resolved, and it is clear that boron incorporation into the framework is minor (only a small fraction of the 0.35 total wt% boron).

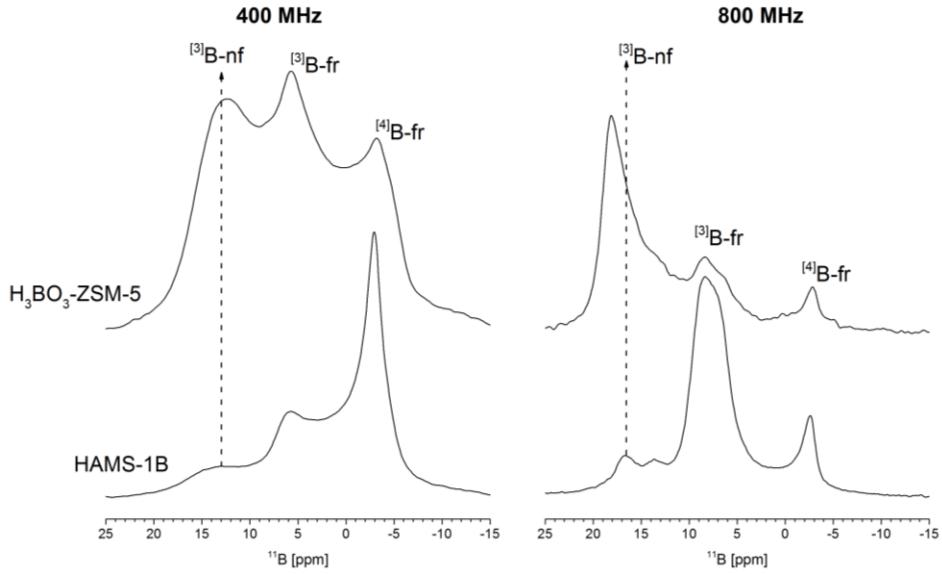

Figure 7. ^{11}B Hahn-echo MAS NMR spectra of boric acid (H_3BO_3)-impregnated ZSM-5 (top) and HAMS-1B (bottom) samples recorded at two distinct magnetic fields. The dashed line depicts the non-framework boron species region.

If boron is so readily removed by slurrying calcined HAMS-1B in distilled water, then why does calcined HAMS-1B have any framework boron in the first place? First, HAMS-1B is synthesized in basic medium under conditions that favor boron insertion as shown in our work. Second, we speculate that the template locks the boron in the framework. Indeed, the ^{11}B Hahn-echo MAS NMR spectrum of as-synthesised HAMS-1B shows only tetrahedral boron framework species (see Fig 8). This figure shows that the trigonal $^{[3]}B$-fr and $^{[3]}B$-nf are formed during drying and calcination and not during sieve synthesis via the pathway shown in Scheme 1.

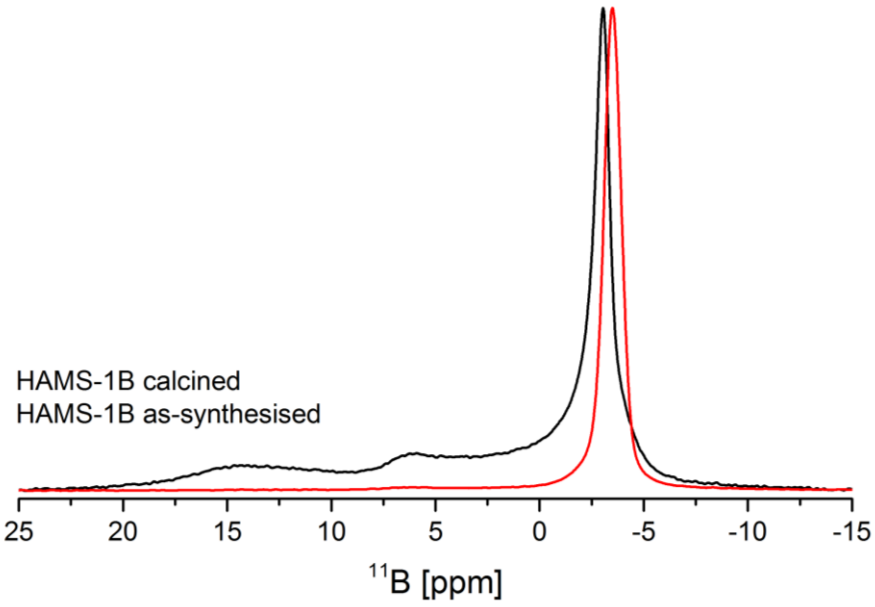

Figure 8. ^{11}B Hahn-echo MAS NMR spectra comparing the as-synthesised (**Red**) and calcined HAMS-1B sieve (**Black**).

4.0 Conclusions

Boron removal from and reinsertion into the framework of a HAMS-1B (H-[B]-ZSM-5) borosilicate molecular sieve was studied by a combination of wet chemistry and ^{11}B solid-state NMR (SSNMR) spectroscopy. Uncalcined HAMS-1B shows only tetrahedral boron. However, three boron species are observed in the NMR spectra of as-prepared and then calcined HAMS-1B-3: tetrahedral framework boron ($^{[4]}B_{fr}$), trigonal framework boron ($^{[3]}B_{fr}$), and non-framework trigonal boron ($^{[3]}B_{NF}$). A picture has emerged as to the origins of these three species. Trigonal boron species are formed via hydrolysis by reaction with the water formed from water release and water formed by oxidation and removal of the template during calcination. $^{[3]}B_{NF}$ is confirmed to be due to free boric acid formed by complete removal of boron from the framework. The trigonal boron species are readily removed from the framework by slurrying in water or mild acid solutions. Tetrahedral boron remains at a concentration about equal to that in the calcined sieve, indicating that it is more difficult to remove. The extent of boron removal and reinsertion is pH dependent. Boron is removed to a greater extent at low pH and can be reinserted when pH is increased. Boron reinsertion into the framework is proven by ^{11}B SSNMR of a series of ^{10}B-^{11}B exchanged borosilicate zeolites. Surprisingly, when boron is reinserted it enters as tetrahedral boron, not trigonal boron, thus reversing partial hydrolysis and removal during calcination.

Acknowedgements

AH gratefully acknowledges funding for her Master's Degree at Cambridge

University from the Kinetics and Catalysis division of the BP Distributed Research Laboratory (DRL).

PVW gratefully acknowledges generous funding from BP Amoco Chemical Company for a postdoctoral stipend plus operating expenses via a special grant from Dr. Charles Cameron, Head of Technology, Downstream, BP, P.L.C.

We are grateful to the Fundação para a Ciência e a Tecnologia (FCT), Fundo Social Europeu and Fundo Europeu de Desenvolvimento Regional (FEDER) for general funding. The authors also thank the Associate Laboratory CICECO (PEst-C/CTM/LA0011/2013), the University of Aveiro, and COMPETE programs for financial support. We also acknowledge the Portuguese NMR Network (RNRMN) for funding. LM greatly thank FCT for the awarded consolidation grant (IF/01401/2013).

References

1. Ch. Baerlocher, Lynne B. McCusker, and D.H. Olson, *Atlas of Zeolite Framework Types, Sixth Edition*, Structure Commission of the International Zeolite Association (2007).
2. P. V. Wiper, J. A. Amelse, and L. Mafra, J. Catal., 316 (2014) 240–250.
3. R. de Ruiter, A.P.M. Kentgens, J. Grootendorst, J. C. Jansen, and H. van Bekkum, *Zeolites*, 13 (1993) 127-138.
4. H. Koller, C. Fild, R.F. Lobo, Microporous Mesoporous Mater. 79 (2005) 215–224.
5. C. Fild, D.F. Shantz, R.F. Lobo, H. Koller, Phys. Chem. Chem. Phys. 2 (2000) 3091–3098.
6. C. Fild, H. Eckert, H. Koller, Angew. Chem. Int. Ed. 37 (1998) 2505–2507.
7. S.-J. Hwang, C.-Y. Chen, and S. I. Zones, *J. Phys. Chem. B*, 108 (2004) 18535–18546.
8. J.A. Amelse, Studies in Surface Science and Catalysis, Proc. North Amer. Meeting of the Catal. Soc., Vol. 38, San Diego, CA, May, 1987.
9. J.A. Amelse, in: 1988 Summer National Meeting of the AIChE, Denver, CO, Aug, (1988).
10. B. L. Meyers, S. R. Ely, N. A. Kutz, and J. A., Kaduk, J. A. *J. Catal.* 91 (1985) 352-355.
11. Y. Seo, K. Cho, Y. Jung, R. Ryoo, ACS Catal. 3 (2013) 713–720.
12. C. Y. Chen and S. I. Zones, Studies in Surface Science and Catalysis, Vol. 135, Proc. of the 13th Intl. Zeolite Conf., Montpellier, France, July, 2001.
13. C. Y. Chen, S. I. Zones, S.-J. Hwang, and L. M. Bull, Studies in Surface Science and Catalysis, Vol.154, 1547-1554 (2004).
14. C.Y. Chen, and S. I. Zones, Zeolites and Catalysis, Synthesis, Reactions and Applications. Vol. 1., 155-170 (2010).
15. S I. Zones, A. Benin, S.-J. Hwang, D. Xie, S. Elomari, and M,-F. Hsieh, JACS, (2014) 136, 1462−1471.
16. J. A. Amelse, A. G. Nerheim, and P.R. Full, Preprints of Poster Papers of the

7th Intl. Zeolite Conf., Poster 3A-7, Tokyo, Japan (1986).
17. J. A. Amelse, A. G. Nerheim, and P. R. Full, Adv. Catal. Chem III: A Symposium in Honor of Prof. M. Boudart, Salt Lake City, UT (1985).